Anisotropic parameter inversion in VTI media using diffraction data

Umair bin Waheed[*†], *Alexey Stovas*[‡], *and Tariq Alkhalifah*[†]
[†] *King Abdullah University of Science and Technology*
[‡] *Norwegian University of Science and Technology*

SUMMARY

Diffracted waves contain useful information regarding the subsurface geometry and velocity. They are particularly valuable for anisotropic media as they inherently possess a wide range of dips necessary to resolve angular dependence of velocity. Using this property of diffraction data to our vantage, we develop an algorithm to invert for effective η model, assuming no prior knowledge of it. The obtained effective η model is then converted to interval η model using Dix-type inversion formula. The effectiveness of this approach is tested on the VTI Marmousi model, which yields good structural match even for a highly complex media such as the Marmousi model.

INTRODUCTION

Diffractions in seismic data contain valuable information that can help improve our velocity model building capability for better imaging of the subsurface. Such information can be used to image geological features beyond the classical Rayleigh limit of half of seismic wavelength (Khaidukov et al., 2004). Inspite of that, diffractions had long been considered as noise in seismic processing and migration. During the last decade, there has been a surge of interest in diffracted waves. The attempts for diffraction imaging, however, have mainly focused on isotropic media. A transverse isotropic (TI) model with vertical symmetry axis (VTI) is one of the most effective approximations to the Earth subsurface. Therefore, diffraction imaging based on the VTI approximation is potentially more accurate than the one based on the isotropic approximation.

In anisotropic media, traveltime computations depend on more than one model parameter. The P-wave traveltimes for VTI media, under the acoustic assumption, depend on the on-axis velocity v_0, the normal-moveout equivalent velocity $v_{nmo} = v_0\sqrt{1+2\delta}$ [where δ is Thomsen parameter (Thomsen, 1986)] and the anellipticity parameter $\eta = \frac{\varepsilon-\delta}{1+2\delta}$ [where ε is also Thomsen parameter (Thomsen, 1986)].

Traveltime computations for VTI media using finite-difference schemes are computationally cumbersome as it entails solving a quartic equation at each time evaluation step. Alkhalifah (2011a) used an elliptical anisotropic model as the starting point for traveltime computation framework based on the perturbation of η in a Taylor series type expansion. This simplification is useful because the elliptical anisotropic model, although represents an uncommon model in practice, has the same order complexity as the isotropic model in terms of solving the eikonal equation. However, since elliptical anisotropy does not provide accurate focusing for media of nonelliptical TI anisotropy, it is used as the background medium for the perturbation expansion. As a result, Alkhalifah (2011b) used perturbation theory to develop traveltime solutions for transverse isotropic media using an elliptical anisotropic model with vertical symmetry axis as the background, thereby requiring perturbation in η.

During the past decades, many of the isotropic time- and depth-migration algorithms have been modified for VTI media. The key issue is to build an accurate velocity model from the data combined with borehole and other sources of information. The anellipticity parameter η can be obtained by inverting either dip-dependent NMO velocity or the hyperbolic reflection moveout (Alkhalifah, 1997b). Then, the η model can be refined in the migrated domain using reflection tomography or migration velocity analysis.

Despite recent successes, medium parameter estimation for heterogeneous TI media remains a highly challenging and unsolved problem. In this paper, we begin by using a scheme to compute traveltimes for the case of a point diffractor using perturbation theory (bin Waheed et al., 2013). Specifically, the source and receiver traveltimes are expanded with regards to a fixed η. This results in a more accurate forward modeling scheme for diffraction data than the simplified isotropic model of the Earth. The accuracy of such a formulation is further enhanced using Shanks transform (Bender and Orszag, 1978). An added advantage of this formulation lies in our ability to use it for inversion of effective η model without the need to compute traveltimes again. The effective η model is then converted to interval η model using Dix-type inversion. We demonstrate the usefulness of our proposed inversion formulation on the VTI Marmousi model (Alkhalifah, 1997a).

THEORY

The 2D eikonal equation in VTI media, under the acoustic assumption, is given as (Alkhalifah, 1998):

$$v_{nmo}^2(1+2\eta)\left(\frac{\partial\tau}{\partial x}\right)^2 + v_0{}^2\left(\frac{\partial\tau}{\partial z}\right)^2\left(1-2\eta v_{nmo}^2\left(\frac{\partial\tau}{\partial x}\right)^2\right) = 1, \quad (1)$$

where $\tau(x,z)$ is the traveltime measured from the source to a point with the coordinates (x,z), v_0 and v_{nmo} are the vertical and NMO velocities measured along the symmetry axis, η denotes the anellipticity parameter.

Numerical solution of equation 1 requires solving a quartic equation at each time step of the finite difference implementation. Therefore, Alkhalifah (2011b) proposed the use of perturbation theory by approximating equation 1 with a series of simpler linear equations. We use an elliptically anisotropic medium as a background model and expand in terms of the parameter η.

The 2D eikonal equation in elliptically anisotropic media (set-

DOI http://dx.doi.org/10.1190/segam2013-0733.1

ting $\eta = 0$ in equation 1) takes the form:

$$v_{nmo}^2 \left(\frac{\partial \tau}{\partial x}\right)^2 + {v_0}^2 \left(\frac{\partial \tau}{\partial z}\right)^2 = 1. \quad (2)$$

The proposed trial solution is:

$$\tau(\eta) \approx \tau_0(x,z) + \tau_1(x,z)\eta(x,z) + \tau_2(x,z)\eta^2(x,z), \quad (3)$$

where τ_0, τ_1 and τ_2 are coefficients of the expansion with dimension of traveltime. For practical purposes, we consider only three terms of the expansion. For a sufficiently smooth η model $\left(\frac{\partial \eta}{\partial x} \ll \beta, \frac{\partial \eta}{\partial z} \ll \beta, \text{ where } \beta \text{ is small}\right)$, the expansion in equation 3 becomes:

$$\tau(\eta) \approx \tau_0(x,z) + \tau_1(x,z)\eta + \tau_2(x,z)\eta^2. \quad (4)$$

Here τ_0 satisfies the elliptically anisotropic eikonal equation 2, whereas τ_1 and τ_2 satisfy linear first-order PDEs having the form:

$$v_{nmo}^2 \frac{\partial \tau_0}{\partial x}\frac{\partial \tau_i}{\partial x} + v_0^2 \frac{\partial \tau_0}{\partial z}\frac{\partial \tau_i}{\partial z} = f_i(x,z), \quad (5)$$

where $i = 1, 2$. The right hand side functions $f_i(x,z)$ depend on terms that can be evaluated sequentially starting with $i = 1$. The exact expressions for the functions $f_1(x,z)$ and $f_2(x,z)$ are given in Alkhalifah (2011a). These right hand side functions become more complicated as we increase the number of terms in the Taylor's series expansion. Therefore, we consider expansion upto second order terms.

However, we can increase the accuracy of expansion in equation 4 by using Shanks transform. Once τ_0, τ_1 and τ_2 have been evaluated, traveltimes can be calculated using the first-sequence of Shanks transform given as:

$$\tau(x,z) \approx \frac{A_0 A_2 - A_1^2}{A_0 - 2A_1 + A_2}, \quad (6)$$

where,

$$A_0 = \tau_0, \qquad A_1 = \tau_0 + \tau_1\,\eta, \qquad A_2 = \tau_0 + \tau_1\,\eta + \tau_2\,\eta^2. \quad (7)$$

This transform tends to predict the behavior of the higher-order terms of the sequence, thereby improving the accuracy of the expansion (Bender and Orszag, 1978).

Plugging in A_0,A_1 and A_2 from equation 7 into equation 6, we get the following traveltime representation:

$$\tau(x,z) \approx \tau_0(x,z) + \frac{\eta\,\tau_1^2(x,z)}{\tau_1(x,z) - \eta\,\tau_2(x,z)}. \quad (8)$$

Let τ_s and τ_r represent expansions in terms of η for traveltimes from source to diffractor and from diffractor to receiver, respectively, then using equation 4, we have:

$$\tau_s(\eta) \approx \tau_{0s} + \tau_{1s}\,\eta + \tau_{2s}\,\eta^2, \quad (9)$$

$$\tau_r(\eta) \approx \tau_{0r} + \tau_{1r}\,\eta + \tau_{2r}\,\eta^2, \quad (10)$$

where τ_{0s}, τ_{1s} and τ_{2s} are coefficients of expansion for source to diffractor wave, while τ_{0r}, τ_{1r} and τ_{2r} denote the expansion coefficients for the wave going from the diffractor to the receiver. Again, using Shanks transform can lead to higher accuracy. By using the transform given by equation 8, we get the following traveltime representation for diffracted wave (bin Waheed et al., 2013):

$$\tau(\eta) \approx (\tau_{0s} + \tau_{0r}) + \frac{\eta\left(\tau_{1s}^2 + \tau_{1r}^2\right)}{(\tau_{1s} + \tau_{1r}) - \eta(\tau_{2s} + \tau_{2r})}. \quad (11)$$

Since the traveltime coefficients are computed using the background elliptically anisotropic inhomogeneous model, equation 11 allows us to invert for the η model without the need for repetitive modeling of traveltimes.

The inverted effective η value is optimal for a particular source and diffractor location. Hence, we represent it by $\widetilde{\eta}_{s_i,d_i}$, where s_i and d_i represent a particular source and diffractor locations, respectively. Considering diffractors located at each grid point in the model, we can obtain the optimal effective η model, denoted by $\widetilde{\eta}_{s_i}(x_d,z_d)$, for a particular source s_i. The coordinates (x_d,z_d) represent diffractor positions in the model.

The cumulative effective η model for several source positions s_i can then be obtained using the relation:

$$\widetilde{\eta}(x_d,z_d) = \frac{1}{N}\sum_{s_i} \widetilde{\eta}_{s_i}(x_d,z_d), \quad (12)$$

where $\widetilde{\eta}(x_d,z_d)$ denotes the cumulative effective η model due to N source locations.

The cumulative effective η model, $\widetilde{\eta}(x_d,z_d)$, can then be converted to an interval η model, denoted by $\eta_i(x_d,z_d)$, using Dix-type inversion formula (Ursin and Stovas, 2005), neglecting lateral variations in parameters:

$$\begin{aligned}(1+8\eta_i)\,v_{0i}^3 &= \frac{\mathrm{d}}{\mathrm{d}z}\left[(1+8\widetilde{\eta})\,\frac{\widetilde{v}_{nmo}^4\,z}{\widetilde{v_0}}\right],\\ \Rightarrow \eta_i &= \frac{1}{8}\left[\frac{\frac{\mathrm{d}}{\mathrm{d}z}\left[(1+8\widetilde{\eta})\,\frac{\widetilde{v}_{nmo}^4 z}{\widetilde{v_0}}\right]}{v_{0i}^3} - 1\right],\end{aligned} \quad (13)$$

where v_{0i} is the interval vertical velocity, and $\widetilde{v_0}$ is the effective vertical velocity, which can be evaluated from v_{0i}, assuming $v(z)$ media, using the relation:

$$\frac{1}{\widetilde{v_0}} = \frac{1}{z}\int_0^z \frac{1}{v_{0i}(\zeta)}\,\mathrm{d}\zeta, \quad (14)$$

whereas $\widetilde{v}_{nmo}$ represents the effective normal moveout velocity given by the relation:

$$\widetilde{v}_{nmo}^2 = \frac{\int_0^z v_{0i}(\zeta)(1+2\delta_i(\zeta))\,d\zeta}{\int_0^z \frac{1}{v_{0i}(\zeta)}\,d\zeta}. \quad (15)$$

NUMERICAL TESTS

In this section, we test the proposed algorithm and use it to obtain the interval η model for the VTI Marmousi model (Alkhalifah, 1997a). The model is interesting due to several faulting and folding features present in both the velocity and η models which may induce diffractions.

DOI http://dx.doi.org/10.1190/segam2013-0733.1

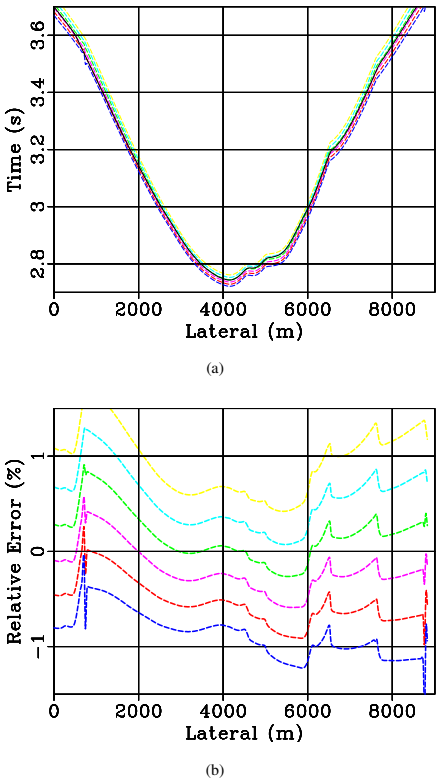

Figure 1: Scanning for effective η values in the Marmousi model for a source located at the center of the experiment surface (4000m,0m). (a) Diffraction traveltime curves observed at the surface and (b) Relative error for these curves obtained for a range of η values from 0 to 0.1 in steps of 0.02 (yellow dashed curve at the top corresponds to $\eta = 0$ while blue dashed curve at the bottom corresponds to $\eta = 0.1$, moving sequentially). Black solid curve in (a) represents the exact diffraction curve. The diffractor considered is located at (4000m,2000m).

First, we consider a diffractor located at (4000m,2000m) in the VTI Marmousi model (see the background model in Figure 2 for the geometry of Marmousi model) and a source located on the surface at the center with coordinates (4000m,0m). Receivers are spread all over the surface of the model. We solve the VTI eikonal equation 1 for a diffraction traveltime curve at the surface using η values given by the model (shown in the background of Figure 2(b)) at each grid point. The computed diffraction traveltime curve is shown in Figure 1(a) (solid black curve). We then assume complete ignorance of the η model and scan for effective η values that best fits this diffraction curve using the formulation given by equation 11. Figure 1(a) also plots the diffraction traveltime curves associated with η ranging from 0 to 0.1 in steps of 0.02. The yellow dashed curve at the top corresponds to $\eta = 0$ while the blue dashed curve in the bottom corresponds to $\eta = 0.1$, moving sequentially. In Figure 1(b) we show relative error associated with these effective η values. Based on this, we can choose the best effective η value for a particular source and diffractor position, $\widetilde{\eta}_{s_i,d_i}$. We then plot traveltime contours in Figure 2 from this diffractor position, comparing our perturbation formulation (dashed curves) with the exact traveltime (solid curves) obtained by solving equation 1. We obtain highly accurate traveltimes, considering that we assumed complete ignorance of the η model and used an effective η obtained after scanning for it.

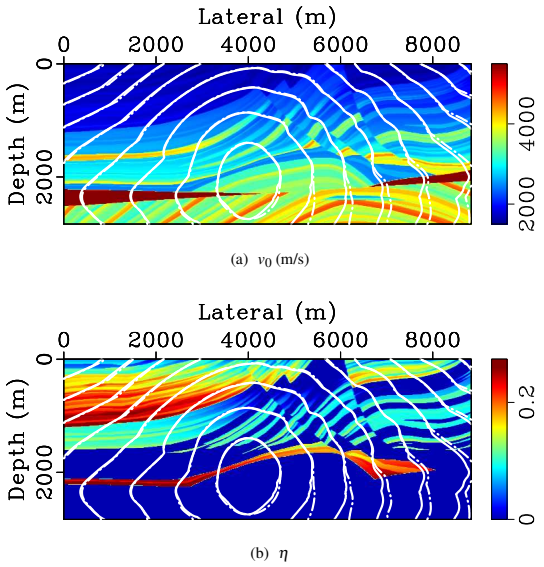

Figure 2: Traveltime contours for the VTI Marmousi model using Shanks transform expansion (dashed) and the exact VTI eikonal solution (solid) mapped on: (a) velocity model and (b) η model. The diffractor considered is located at (4000m,2000m). The exact solution uses η values given by the model in (b) at each grid point while Shanks transform expansion uses an effective η value.

By considering a diffractor located at each grid point, we obtain the best effective value, $\widetilde{\eta}_{s_i,d_i}$, for all points in the model, keeping the source location fixed at (4000m,0m). Figure 3(a) shows the optimal effective η model for this source location. The effective η values are then converted to interval η values using equation 13, shown in Figure 3(b).

As Figure 3 was obtained using illumination due to a single source, the inverted η model is not well resolved in certain areas. Therefore, next we consider nine equispaced sources on the surface and repeat the afore-mentioned procedure. Having obtained the optimal effective η model for each source, $\widetilde{\eta}_{s_i}$, we obtain cumulative effective η model for all sources, $\widetilde{\eta}$ using equation 12, shown in Figure 4(a). This is then used to obtain inverted η model using equation 13. As can be seen by comparing Figures 3 and 4, there is a considerable improvement in the inverted η model using more sources due to illumination from different angles.

We also present the cumulative effective η and the interval η model for seventeen equispaced sources in Figure 5, which shows an even improved image. The resultant interval η seems smother and more accurate.

DOI http://dx.doi.org/10.1190/segam2013-0733.1

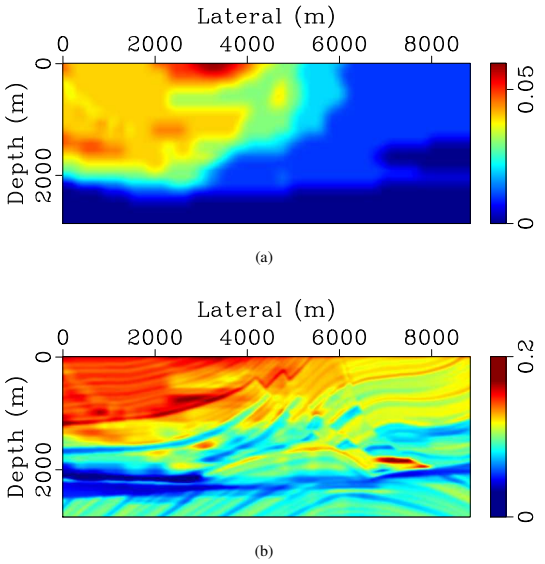

Figure 3: (a) Effective η model and (b) Interval η model obtained for the VTI Marmousi model using a single source located at (4000m,0m).

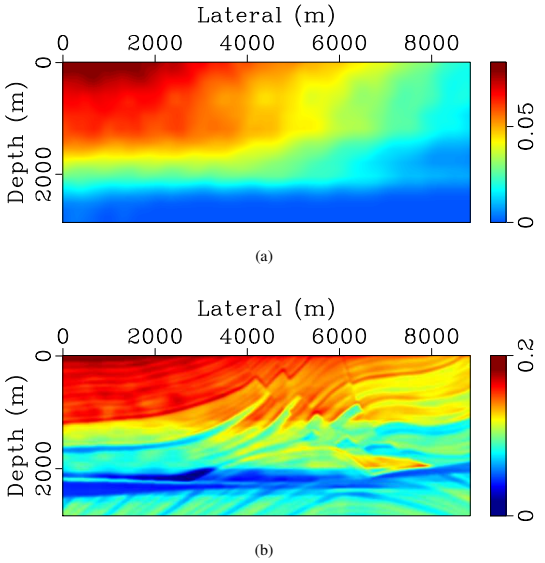

Figure 4: (a) Cumulative effective η model and (b) Interval η model obtained for the VTI Marmousi model using nine equispaced sources on the surface.

DISCUSSION

The detailed interval η model was obtained from a combination of considering every point in the model a diffractor and having a detailed accurate velocity model in the background. In practice, such information surely will not be available, however, the approach demonstrates how we can manipulate our interval η distribution to comply with the structure of the interval velocity used in the background, whether it is accurate or not, and whether it is high resolution or smooth. Of course, reliable diffractions are present in certain locations, not every grid point, though many recently (Fomel et al., 2007; Klokov and Fomel, 2012), through effective diffraction separation methods, obtain sections of real data with very large number of diffractions that usually do not appear in the conventional reflection section. Of course, fewer diffractions will lower the resolution of the effective η estimation, but effective η is overall smooth, and thus the lower number of measurements will have a reduced effect. The formulation considers knowledge of the vertical velocity model. However, we aim to study the sensitivity of the inverted η model to imperfect knowledge of velocity model. Results of such tests will also be presented at the SEG 83rd annual meeting.

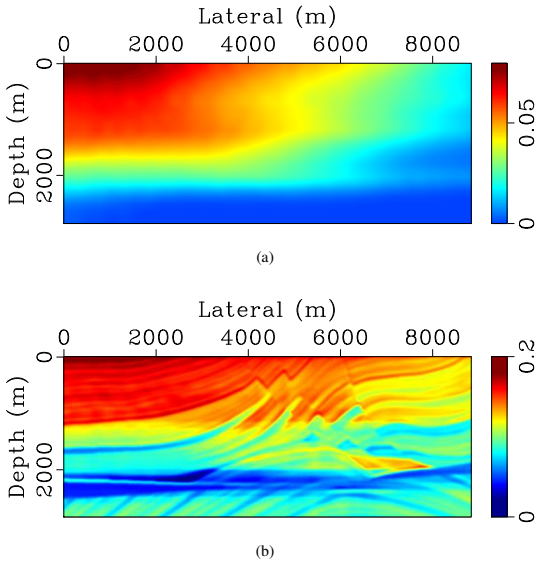

Figure 5: (a) Cumulative effective η model and (b) Interval η model obtained for the VTI Marmousi model using seventeen equispaced sources on the surface.

CONCLUSION

We develop a procedure to use diffraction traveltimes to invert for the interval η model, assuming no prior knowledge of it. The inverted effective η produces traveltimes that match very much the measured ones, even in the complex Marmousi model. The results demonstrate a good structural match between the original and inverted η model, granted we have an accurate background velocity, even for a few source positions. As the number of sources increase, the inverted model is expected to converge better to the original model.

ACKNOWLEDGMENTS

We would like to thank KAUST and ROSE project for financial support.

DOI http://dx.doi.org/10.1190/segam2013-0733.1

REFERENCES

Alkhalifah, T., 1997a, Anisotropic marmousi data set: Stanford Exploration Project-95, 265–282.

———, 1997b, Seismic data processing in vertically inhomogeneous TI media: Geophysics, **62**, 662–675.

———, 1998, Acoustic approximations for processing in transversely isotropic media: Geophysics, **63**, 623–631.

———, 2011a, Scanning anisotropy parameters in complex media: Geophysics, **76**, U13–U22.

———, 2011b, Traveltime approximations for transversely isotropic media with an inhomogeneous background: Geophysics, **76**, WA31–WA42.

Bender, C. M., and S. A. Orszag, 1978, Advanced mathematical methods for scientists and engineers: McGraw-Hill.

bin Waheed, U., T. Alkhalifah, and A. Stovas, 2013, Diffraction traveltime approximations for TI media with an inhomogeneous background: Geophysics, submitted.

Fomel, S., E. Landa, and M. T. Taner, 2007, Poststack velocity analysis by separation and imaging of seismic diffractions: Geophysics, **72**, U89–U94.

Khaidukov, V., E. Landa, and T. J. Moser, 2004, Diffraction imaging by focusing-defocusing: An outlook on seismic superresolution: Geophysics, **69**, 1478–1490.

Klokov, A., and S. Fomel, 2012, Separation and imaging of seismic diffractions using migrated dip-angle gathers: Geophysics, **77**, S131.

Thomsen, L., 1986, Weak elastic anisotropy: Geophysics, **51**, 1954–1966.

Ursin, B., and A. Stovas, 2005, Generalized Dix equations for a layered transversely isotropic medium: Geophysics, **70**, 77–81.

DOI http://dx.doi.org/10.1190/segam2013-0733.1

http://dx.doi.org/10.1190/segam2013-0733.1

EDITED REFERENCES

Note: This reference list is a copy-edited version of the reference list submitted by the author. Reference lists for the 2013 SEG Technical Program Expanded Abstracts have been copy edited so that references provided with the online metadata for each paper will achieve a high degree of linking to cited sources that appear on the Web.

REFERENCES

Alkhalifah, T., 1997a, Anisotropic marmousi data set: Stanford Exploration Project, **95**, 265–282.

Alkhalifah, T., 1997b, Seismic data processing in vertically inhomogeneous TI media: Geophysics, **62**, 662–675, http://dx.doi.org/10.1190/1.1444175.

Alkhalifah, T., 1998, Acoustic approximations for processing in transversely isotropic media: Geophysics, **63**, 623–631, http://dx.doi.org/10.1190/1.1444361.

Alkhalifah, T., 2011a, Scanning anisotropy parameters in complex media: Geophysics, **76**, no. 2, U13–U22, http://dx.doi.org/10.1190/1.3553015.

Alkhalifah, T., 2011b, Traveltime approximations for transversely isotropic media with an inhomogeneous background: Geophysics, **76**, no. 3, WA31–WA42, http://dx.doi.org/10.1190/1.3555040.

Bender, C. M., and S. A. Orszag, 1978, Advanced mathematical methods for scientists and engineers: McGraw-Hill.

Fomel, S., E. Landa, and M. T. Taner, 2007, Poststack velocity analysis by separation and imaging of seismic diffractions: Geophysics, **72**, no. 6, U89–U94, http://dx.doi.org/10.1190/1.2781533.

Khaidukov, V., E. Landa, and T. J. Moser, 2004, Diffraction imaging by focusing-defocusing: An outlook on seismic superresolution: Geophysics, **69**, 1478–1490, http://dx.doi.org/10.1190/1.1836821.

Klokov, A., and S. Fomel, 2012, Separation and imaging of seismic diffractions using migrated dip-angle gathers: Geophysics, **77**, no. 6, S131–S143, http://dx.doi.org/10.1190/geo2012-0017.1.

Thomsen, L., 1986, Weak elastic anisotropy: Geophysics, **51**, 1954–1966, http://dx.doi.org/10.1190/1.1442051.

Ursin, B., and A. Stovas, 2005, Generalized Dix equations for a layered transversely isotropic medium: Geophysics, **70**, 77–81.